

## Resonant, direct, and transfer breakup of ${}^6\text{Li}$ by ${}^{112}\text{Sn}$

D. Chattopadhyay,<sup>1,2</sup> S. Santra,<sup>1,2,\*</sup> A. Pal,<sup>1,2</sup> A. Kundu,<sup>1,2</sup> K. Ramachandran,<sup>1</sup> R. Tripathi,<sup>2,3</sup> D. Sarkar,<sup>1</sup> S. Sodaye,<sup>2,3</sup>  
B. K. Nayak,<sup>1,2</sup> A. Saxena,<sup>1,2</sup> and S. Kailas<sup>1,2</sup>

<sup>1</sup>Nuclear Physics Division, Bhabha Atomic Research Centre, Mumbai 400085, India

<sup>2</sup>Homi Bhabha National Institute, Anushakti Nagar, Mumbai - 400094, India

<sup>3</sup>Radio Chemistry Division, Bhabha Atomic Research Centre, Mumbai 400085, India

(Received 17 October 2016; revised manuscript received 22 November 2016; published 27 December 2016)

Projectile breakup cross sections in the  ${}^6\text{Li}+{}^{112}\text{Sn}$  reaction have been measured at two beam energies, 30 and 22 MeV. Cross sections for sequential breakup of  ${}^6\text{Li}$  into  $\alpha + d$  via its resonant state of  $1^+$  (5.65 MeV) in the continuum have been measured for the first time along with two other dominant resonant states of  $3^+$  (2.18 MeV) and  $2^+$  (4.31 MeV) at  $E_{\text{beam}} = 30$  MeV. However, at 22 MeV, the  $\alpha + d$  breakup is found to be only due to direct breakup process. Cross sections measured for sequential breakup via two transfer channels, ( ${}^6\text{Li}, {}^5\text{Li}$ ) and ( ${}^6\text{Li}, {}^8\text{Be}$ ), into  $\alpha + p$  and  $\alpha + \alpha$ , respectively, and the above  $\alpha + d$  breakup channels compared with the results of coupled-channels calculations unravel the reaction mechanisms involving a weakly bound projectile and different processes leading to large inclusive  $\alpha$ -particle production.

DOI: [10.1103/PhysRevC.94.061602](https://doi.org/10.1103/PhysRevC.94.061602)

The study of nuclear reactions involving weakly bound projectiles has been drawing tremendous interests due to the observation of many new features compared to the ones involving strongly bound projectiles. Suppression in complete fusion (CF) cross sections [1], breakup threshold anomaly in the optical potentials obtained from elastic scattering [2], and high yield in  $\alpha$  particle production [3] are some of the interesting features. The presence of projectile breakup channels in addition to other nonelastic channels and their coupling to the elastic channel are the prime factors behind the above differences. Several measurements in the literature have focused on identifying different breakup channels and estimating their cross sections. In a systematic work by Pfeiffer *et al.* [4], it has been observed that the yield of  $\alpha$  particles measured in reactions involving a  ${}^6\text{Li}$  beam with several targets ( ${}^{58}\text{Ni}$ ,  ${}^{118,120}\text{Sn}$ , and  ${}^{208}\text{Pb}$ ) is unexpectedly large and the production cross section at an energy normalized to the Coulomb barrier is independent of the target. The observation of smaller cross sections for deuterons compared to  $\alpha$  particles suggested the existence of other competing processes with  $\alpha$  particles in the exit channel, such as transfer reactions leading to  $\alpha$  unstable  ${}^5\text{He}$  or  ${}^5\text{Li}$  or excitation of quasicontinuously neighbored states by multinucleon transfer. It was also concluded that these additional processes are more important at sub- and near-barrier energies than anticipated. Particle-particle correlation measurements in  ${}^6\text{Li}+{}^{208}\text{Pb}$  [5] and  ${}^6\text{Li}+{}^{118}\text{Sn}, {}^{208}\text{Pb}$  [6] reactions at near barrier energies confirmed the presence of not only the direct breakup of  ${}^6\text{Li} \rightarrow \alpha + d$  but also the sequential breakup via one of its resonance states [i.e.,  ${}^6\text{Li} \rightarrow {}^6\text{Li}^*(3^+) \rightarrow \alpha + d$ ] and transfer induced breakup like  ${}^6\text{Li} \rightarrow {}^5\text{Li} \rightarrow \alpha + p$  and  ${}^6\text{Li} \rightarrow {}^8\text{Be} \rightarrow \alpha + \alpha$ . In a detailed investigation by Castaneda *et al.* for the  ${}^6\text{Li}+{}^{197}\text{Au}$  reaction [7], the sequential breakup via first resonant state of  ${}^6\text{Li}$  (i.e.,  $3^+$ , 2.18 MeV) and  $1n$  transfer followed by breakup (i.e.,  ${}^6\text{Li} \rightarrow {}^5\text{Li} \rightarrow \alpha + p$ ) was again

observed. A similar observation was made by Signorini *et al.* [8,9] in  ${}^6\text{Li}+{}^{208}\text{Pb}$  reaction. In reactions  ${}^7\text{Li}+{}^{197}\text{Au}$  [10] and  ${}^7\text{Li}+{}^{65}\text{Cu}$  [11],  $1n$  stripping transfer followed by breakup of  ${}^6\text{Li}$  via its first resonance state ( $3^+$ , 2.18 MeV) was observed. While, in the case of the  ${}^6\text{Li}+{}^{65}\text{Cu}$  reaction [11], the breakup of  ${}^6\text{Li}$  via its first ( $3^+$ , 2.18 MeV) as well as second resonance ( $2^+$ , 4.31 MeV) states were observed. These studies show that the probability of breakup of the clustered projectiles or projectile-like fragments, such as  ${}^{6,7}\text{Li}$ , into two or more fragments proceeding through their resonance states is quite large. Therefore, for the  ${}^6\text{Li}$  case, one can expect its breakup through all three resonance states corresponding to  $L = 2$ , i.e., ( $3^+$ , 2.18 MeV), ( $2^+$ , 4.31 MeV), and ( $1^+$ , 5.65 MeV) [12,13]. So far there is no study available in the literature on the experimental breakup cross sections for  ${}^6\text{Li}$  via its  $1^+$  resonance state. Since the excitation energy and width of this state is very large, the cross section is expected to be less compared to the other two ( $2^+$  and  $3^+$ ) resonance states. Also, since the relative energy of the breakup fragments proceeding via this resonance state is large (4.18 MeV), the detection cone angle is expected to be large requiring a bigger detector system. However, it would be interesting and challenging to measure the breakup cross section via this state along with the other two states using a detector setup covering a large solid angle and find their relative contributions.

In a recent study on breakup reactions in the  ${}^7\text{Li}+{}^{93}\text{Nb}$  system [14], at energies around the Coulomb barrier, the importance of transfer breakup, viz.  $1p$  pickup and  $1n$  stripping, to unbound states of the ejectile followed by its breakup compared to direct breakup of the projectile have been explored. In the measurements by Luong *et al.* [15] for  ${}^6\text{Li} + {}^{208}\text{Pb}, {}^{209}\text{Bi}$  reactions at sub-barrier energy, it has been observed that the probability of  $1n$  transfer followed by breakup, i.e.,  ${}^6\text{Li} \rightarrow {}^5\text{Li} \rightarrow \alpha + p$ , is always greater than the inelastic breakup, i.e.,  ${}^6\text{Li} \rightarrow {}^6\text{Li}^*(3^+) \rightarrow \alpha + d$ , for both the reactions. These breakup phenomena can be further probed involving  ${}^6\text{Li}$  as a projectile with a different target ( ${}^{112}\text{Sn}$ ) to confirm the target independence if any. It would also be

\*ssantra@barc.gov.in

interesting to see the energy dependence of these breakup probabilities.

This Rapid Communication presents the results of exclusive measurements of different breakup channels in the  ${}^6\text{Li}+{}^{112}\text{Sn}$  reaction at two beam energies. Continuum-discretized-coupled-channels (CDCC) and coupled-reaction-channels (CRC) calculations are performed to understand the experimental cross sections for both direct as well as sequential breakup (through resonance states of  ${}^6\text{Li}$  and transfer reactions). Experimental and/or theoretical cross sections have been compared to disentangle the individual contributions to inclusive  $\alpha$  production and understand the underlying reaction mechanism.

Exclusive measurements have been carried out for the  ${}^6\text{Li}+{}^{112}\text{Sn}$  reaction at two beam energies, 22 and 30 MeV, using the 14-UD Pelletron-Linac facility in Mumbai. A self-supporting enriched  ${}^{112}\text{Sn}$  target of thickness  $\approx 540 \mu\text{g}/\text{cm}^2$  has been used. The cone angles between two possible breakup fragments ( $\alpha$  and  $d$  or  $\alpha$  and  $p$  or  $\alpha$  and  $\alpha$ ) of the projectile/ejectile ( ${}^6\text{Li}$  or  ${}^5\text{Li}$  or  ${}^8\text{Be}$ ) through their ground as well as excited states are estimated to be in the range of  $6^\circ$ – $56^\circ$ . Being interested in all the above breakup channels, four sets of strip telescopes placed side by side covering a total angular range of  $\sim 76^\circ$  have been used inside a 1.5-m diameter scattering chamber to detect different breakup fragments in coincidence. Each strip telescope consists of two double-sided Si strip detectors, with thickness of  $\sim 50$ – $60 \mu\text{m}$  (as  $\Delta E$ ) and  $1500 \mu\text{m}$  (as  $E$ ), respectively. Each detector has 16 vertical strips in its front side and 16 horizontal strips in its back side covering an active area of  $50 \text{ mm} \times 50 \text{ mm}$ . Two Si surface barrier detectors ( $M_1$  and  $M_2$ ) of thickness 1 mm were placed at  $\pm 20^\circ$  with respect to the beam direction for normalization and beam monitoring. In addition, there were five telescopes of single surface barrier detectors (with  $\Delta E \sim 50 \mu\text{m}$  and  $E \sim 1000$ – $2000 \mu\text{m}$ ) placed on the second arm of the scattering chamber to measure elastic and inclusive  $\alpha$  cross sections at the remaining angles as well as some overlapping angles to compare their data with the ones from strip detectors. The inclusive two-dimensional raw spectra of  $\Delta E$  versus  $E_{\text{res}}$  signals shows good separation of the particles with different masses as shown in Fig. 1.

In the event-by-event mode off-line analysis, the coincidence yields in any two strips with  $\alpha$  particles in one strip and dominant fragments like deuterons or protons or  $\alpha$  particles in any other strip have been extracted independently by employing two-dimensional gates in respective particle bands obtained from the strip telescopes. The  $Q$ -value spectra, generated using the relation given in Ref. [15], for  $\alpha + d$ ,  $\alpha + p$ , and  $\alpha + \alpha$  breakup channels at  $E_{\text{beam}} = 30$  as well as 22 MeV are shown in Figs. 2(a), 2(c), and 2(e), respectively. The figure provides information on breakup probabilities corresponding to different excitations of the intermediate or outgoing (projectile-like or target-like) particles. In Fig. 2(a), for  $\alpha + d$  breakup at  $E_{\text{beam}} = 30$  MeV (shown in red color), three peaks in the  $Q$ -value spectrum at 2.18 MeV, 4.31 MeV, and 5.65 MeV correspond to the resonance excitations of  ${}^6\text{Li}$  at  $3^+$ ,  $2^+$ , and  $1^+$  states, respectively, implying sequential breakup is dominant at  $E_{\text{beam}} = 30$  MeV. To our knowledge this is the first observation of  $\alpha - d$  breakup via the  $1^+$

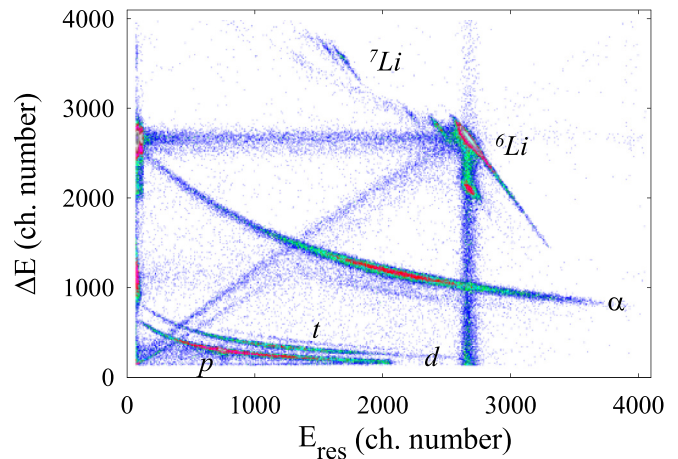


FIG. 1. A typical two-dimensional raw spectrum of a vertical strip placed at  $51^\circ$ .

resonance state of  ${}^6\text{Li}$  in addition to its already known  $3^+$  and  $2^+$  resonance states. The direct breakup of  ${}^6\text{Li}$  via its nonresonant states have also been observed. The  $1n$  stripping reaction followed by breakup into  $\alpha + p$ , as shown in Fig. 2(c), is preferred via the ground state of  ${}^5\text{Li}$  and  ${}^{113}\text{Sn}$ , but several excitations of  ${}^{113}\text{Sn}$  are also observed. Whereas, the  $1d$  pickup reaction followed by  $\alpha + \alpha$  breakup, as shown in Fig. 2(e), is

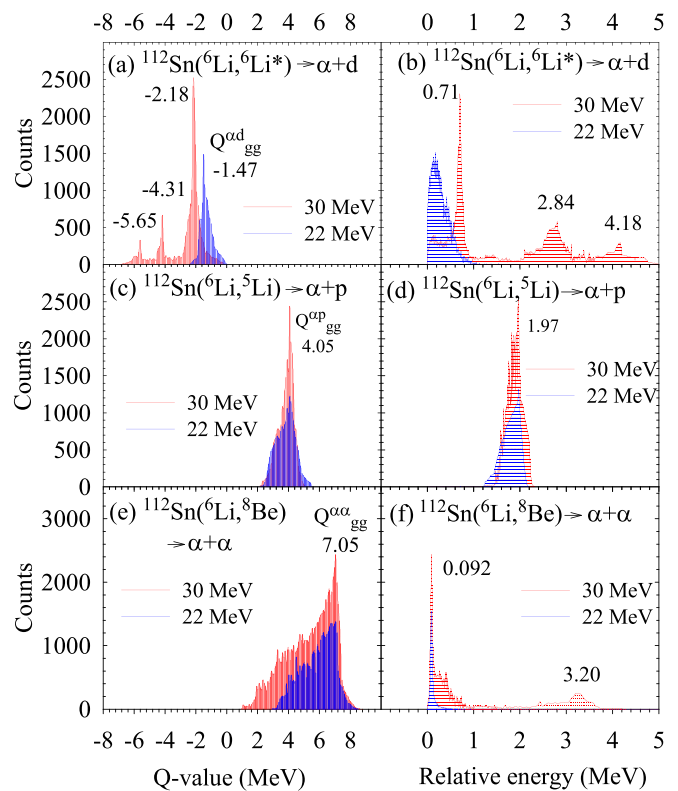


FIG. 2. Comparison of the yield distributions of  $\alpha - d$ ,  $\alpha - p$ , and  $\alpha - \alpha$  breakup as a function of  $Q$  value and relative energy at two different beam energies, i.e., 22 and 30 MeV.

found to proceed via both ground state ( $0^+$ ) as well as excited state ( $2^+$ , 3.02 MeV) of  $^8\text{Be}$  and several excited states of  $^{110}\text{In}$ .

The coincidence spectra have also been built as a function of relative energies of two breakup fragments as defined in Ref. [16] and shown in Figs. 2(b), 2(d), and 2(f) in order to find out excitation energies above the breakup threshold of the intermediate projectile-like particles like  $^6\text{Li}$ ,  $^5\text{Li}$ ,  $^8\text{Be}$ , etc. Similar to  $Q$ -value spectra, the breakup yield of  $^6\text{Li} \rightarrow \alpha + d$  at  $E_{\text{beam}} = 30$  MeV is found to peak at relative energies equal to excitations corresponding to the resonance states of  $^6\text{Li}$  [see Fig. 2(b)]. This confirms not only the dominance of sequential  $\alpha + d$  breakup but also the observation of breakup via the  $1^+$  resonance state of  $^6\text{Li}$  along with its  $3^+$  and  $2^+$  resonance states. For  $^6\text{Li} \rightarrow ^5\text{Li} \rightarrow \alpha + p$  breakup, as shown in Fig. 2(d), the yield has a broad peak for  $\alpha$ - $p$  relative energy  $E_{\alpha p} \sim 1.97$  MeV which is equal to the g.s.  $Q$  value in  $^5\text{Li} \rightarrow \alpha + p$  breakup. In the case of  $^6\text{Li} \rightarrow ^8\text{Be} \rightarrow \alpha + \alpha$  breakup, as shown in Fig. 2(f), the yield is maximum at  $E_{\alpha\alpha} = 0.092$  MeV (the g.s.  $Q$  value in  $^8\text{Be} \rightarrow \alpha + \alpha$  reaction). A small peak in the  $\alpha + \alpha$  breakup yield at  $E_{\alpha\alpha} \sim 3.2$  MeV corresponds to the excitation energy due to breakup via the first excited state ( $2^+$ ) of  $^8\text{Be}$ .

In order to find the beam energy dependence of the direct and sequential breakup contributions, the above measurements were repeated at another beam energy,  $E_{\text{beam}} = 22$  MeV, around the Coulomb barrier. The  $Q$ -value spectra and relative energy spectra for  $\alpha + d$ ,  $\alpha + p$ , and  $\alpha + \alpha$  breakup for both beam energies, i.e., 22 and 30 MeV, have been compared in Fig. 2. It is interesting to observe that the breakup of  $^6\text{Li} \rightarrow \alpha + d$  at  $E_{\text{beam}} = 22$  MeV now proceeds only through direct breakup. No sequential  $\alpha + d$  breakup peak is observed. This may be due to lower beam energy (22 MeV) which is slightly higher than the Coulomb barrier ( $V_b \sim 21$  MeV) but less than the breakup threshold. In the case of  $\alpha + p$  breakup, as shown in Figs. 2(c), 2(d), the shapes of the  $Q$ -value spectra as well as the relative energy spectra at two beam energies are similar, implying that this channel proceeds through the same states of  $^5\text{Li}$  and  $^{113}\text{Sn}$  at both energies. Finally, for the  $\alpha + \alpha$  case, as shown in Figs. 2(e), 2(f), the breakup of  $^8\text{Be}$  at 22 MeV is found to proceed mainly through its ground state ( $0^+$ ). However, at 30 MeV, the breakup proceeds through both the ground state as well as the first excited state ( $2^+$ ) of  $^8\text{Be}$ .

Similar to the observation earlier [17], the yields of the two peaks [6,7] corresponding to the sequential  $\alpha + d$  breakup through a particular resonance state of  $^6\text{Li}^*$  are also found to be asymmetric for the present reaction. The  $\alpha$ - $d$  coincidence yields under the two peaks corresponding to the same relative energy have been used separately to calculate the differential breakup cross sections in the center-of-mass system at various angles using the formulation of Ref. [16] and Jacobian factors [18] of the transformation. The two peaks in each of  $\alpha$  or  $d$  coincident spectra correspond to two center-of-mass angles of  $^6\text{Li}^*$  [6,7] which are slightly different in the case of  $3^+$  and  $2^+$  resonant breakup. An average of the cross sections obtained from the two (low and high energy) peaks of particular coincidence spectrum has been obtained for each of  $3^+$  and  $2^+$  breakup and the results are shown in Fig. 3. However, for  $1^+$  breakup, the cross sections obtained for each of the two coincidence peaks have been plotted independently

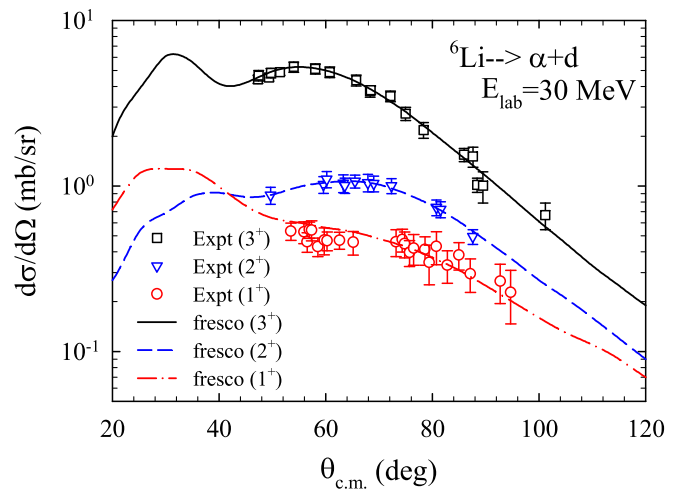


FIG. 3. Sequential  $\alpha + d$  breakup cross section in center-of-mass frame measured at 30 MeV. See text for details.

as the difference in center-of-mass angles corresponding to two peaks is large ( $12^\circ$ – $22^\circ$ ). Differential cross sections for sequential  $\alpha + d$  breakup via  $3^+$ ,  $2^+$ , and  $1^+$  resonances shown in Fig. 3 are represented by squares, triangles, and circles, respectively. Although the resonant breakup cross sections via  $3^+$  and  $2^+$  states of  $^6\text{Li}$  in reactions involving a few targets have been measured and described earlier, the cross section for  $1^+$  state is measured for the first time in the present reaction. The lines plotted in the above figure, representing theoretical calculations as described later, explain the experimental cross sections very well and thus support the observation of above resonant breakups.

Using the formulation of Ref. [16] and assuming isotropic emissions of the fragments, the experimental differential cross sections for direct breakup of  $^6\text{Li} \rightarrow \alpha + d$  have been extracted and shown in Figs. 4(a) and 4(b). At  $E_{\text{beam}} = 30$  MeV, the coincident  $\alpha + d$  breakup yields with relative energies in the range of  $E_{\alpha d} = 0$ –2 MeV, excluding the contributions of sequential breakup of the resonant states, are used. For  $E_{\text{beam}} = 22$  MeV, no significant contribution from the resonant states has been observed experimentally. So, the  $\alpha + d$  breakup yields covering the measured range of relative energies, i.e.,  $E_{\alpha d} = 0$  to 1.4 MeV, have been considered for direct breakup cross section estimations. The results of FRESKO calculations including projectile inelastic excitations up to the same limit as measured in the experiment, represented by solid lines, explain the experimental data very well. Calculations for direct breakup with  $\alpha d$  excitations up to a maximum of 8 MeV which is included in full CDCC calculations are represented by dashed lines for both beam energies.

The elastic scattering cross sections calculated simultaneously using the same cluster-folded potential with breakup couplings, represented by dash-dotted lines are also compared with the experimental data (diamonds) in Figs. 4(c) and 4(d) for 30 and 22 MeV, respectively.

As observed in Fig. 2, the two major channels of transfer reactions followed by breakup are  $^6\text{Li} \rightarrow ^5\text{Li} \rightarrow \alpha + p$  and  $^6\text{Li} \rightarrow ^8\text{Be} \rightarrow \alpha + \alpha$ . The yields in  $\alpha$ - $p$  and  $\alpha$ - $\alpha$  coincidences are of the same order as that of  $\alpha$ - $d$  coincidence for any

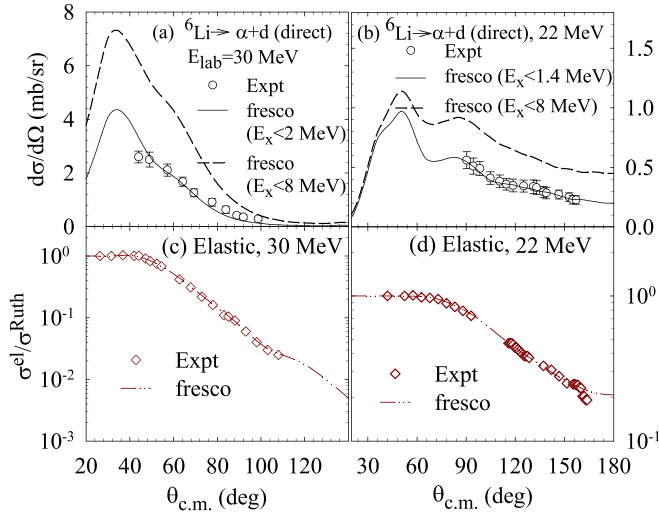


FIG. 4. Differential cross sections for direct breakup of  ${}^6\text{Li} \rightarrow \alpha + d$  in center-of-mass frame measured at  $E_{\text{beam}}$  of (a) 30 MeV and (b) 22 MeV. (c), (d) Measured elastic scattering angular distribution (diamonds) at respective energies along with the result of CDCC calculations (dash-dot-dot lines). See text for details.

particular energy. Thus these two breakup channels along with the  $\alpha + d$  channel are expected to have significant contributions to the total  $\alpha$  particle production in the reaction. Assuming isotropic emission of the breakup fragments in the center-of-mass frame and using the formulation of Ref. [16], experimental cross sections for  $\alpha + p$  and  $\alpha + \alpha$  breakup have been extracted and shown in Figs. 5(a) and 5(b), respectively.

Breakup cross sections for  ${}^6\text{Li} \rightarrow \alpha + d$  have been calculated by the continuum discretized coupled channels (CDCC) method using FRESKO [19] similar to the one described in Ref. [17]. The cluster-folded (CF) interaction [20] with  $V_{\alpha+Sn}$  potential from Ref. [21] at  $E_{\text{beam}} = 19.5$  MeV and  $V_{d+Sn}$  potential at  $E_{\text{beam}} = 10$  MeV from the global fit [22] have been used. Results of the CDCC calculations for two beam energies, 30 and 22 MeV, are shown in Figs. 3 and 4. In Figs. 4(c) and 4(d), the calculated elastic scattering angular distributions (lines) reproduce the experimental data (diamonds) well. The

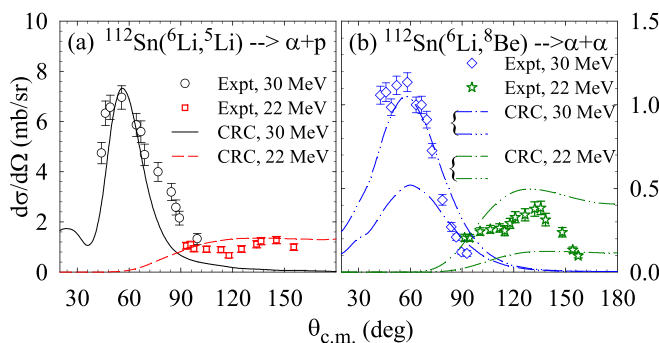


FIG. 5. Differential cross sections in center-of-mass frame for sequential breakup of (a)  ${}^6\text{Li} \rightarrow {}^5\text{Li} \rightarrow \alpha + p$ , and (b)  ${}^6\text{Li} \rightarrow {}^8\text{Be} \rightarrow \alpha + \alpha$  measured at  $E_{\text{beam}} = 30$  MeV and 22 MeV. Lines represent CRC calculations (see text for details).

breakup cross sections calculated for three resonant states ( $3^+$ ,  $2^+$ , and  $1^+$ ) shown, respectively, as solid, dashed, and dash-dotted lines in Fig. 3 explain the experimental data very well.

Coupled reaction channels (CRC) calculations using FRESKO for  $1n$  stripping and  $1d$  pickup reactions have been compared with the measured  $\alpha + p$  and  $\alpha + \alpha$  breakup cross sections. When the ejectiles  ${}^5\text{Li}$  and  ${}^8\text{Be}$  formed in the above transfer reactions are unstable to the above breakup channels, the transfer cross sections are assumed to be equal to breakup cross sections. For the entrance and exit channels of CRC calculations, the real potential obtained from the fit to measured elastic scattering was used. But the imaginary potentials were of short range and Woods-Saxon square form. In the case of the  $1n$  stripping reaction, the ground state of  ${}^5\text{Li}$  and ground plus six excited states of  ${}^{113}\text{Sn}$  have been included. Spectroscopic factors for  $\langle {}^{112}\text{Sn} + n | {}^{113}\text{Sn} \rangle$  corresponding to seven states ( $E_x = 0-1.556$  MeV) of  ${}^{113}\text{Sn}$  are taken from Ref. [23]. Spectroscopic factors for  $\langle {}^6\text{Li} | {}^5\text{Li} + n \rangle$  is assumed to be 0.56 to reproduce the experimental data. Results are shown in Fig. 5(a) as solid and dashed lines corresponding to 30 and 22 MeV, respectively. In the case of the  $1d$  pickup reaction, the possibility of both single step transfer as well as double step ( $1p$  followed by  $1n$  or vice versa) transfers have been considered. The  $0^+$  and  $2^+$  state of  ${}^8\text{Be}$  and ground plus first two excited states of  ${}^{110}\text{In}$  have been coupled. These are only a few representative states out of many excitations of  ${}^{110}\text{In}$  as observed in Fig. 2(e). Spectroscopic factors for  $\langle {}^6\text{Li} + p | {}^7\text{Be} \rangle$  are taken to be the same as  $\langle {}^6\text{Li} + n | {}^7\text{Li} \rangle$  [24] and those for  $\langle {}^{111}\text{Sn} + n | {}^{112}\text{Sn} \rangle$  are taken from Ref. [25]. The other overlaps which are not available in the literature are assumed to be 1.0. Calculated cross sections with only g.s. (dash-dot line) and ground plus excited states of  ${}^{110}\text{In}$  (dash-dot-dot line) shown in Fig. 5(b) reproduce the peak positions of the experimental data.

As observed earlier for several reactions (Ref. [3] and references therein), a large number of  $\alpha$  particles is also produced for the present system. From the measured inclusive  $\alpha$  angular distributions (not shown here) the angle integrated cross sections for 30 and 22 MeV have been tabulated in Table I. A comprehensive list of experimental and/or theoretical cross sections corresponding to different channels

TABLE I. Experimental and calculated cross sections for various channels at  $E_{\text{beam}} = 30$  and 22 MeV.

Reaction channel	$\sigma_{30}(\text{mb})$ (expt.)	(theory)	$\sigma_{22}(\text{mb})$ (expt.)	(theory)
Inclusive breakup- $\alpha$	$592 \pm 35$	—	$309 \pm 16$	—
${}^6\text{Li}^* \rightarrow \alpha + d$ (resonant)	$34 \pm 4$	34.6	—	15.2
${}^6\text{Li} \rightarrow \alpha + d$ (direct)	$12 \pm 2.0^a$	$12^a$	$6 \pm 1^b$	$6.1^b$
	—	$25.9^c$	—	$9.3^c$
${}^6\text{Li} \rightarrow \alpha + d$ (total)	$46 \pm 4.5$	60.5	$6 \pm 1^b$	24.5
${}^6\text{Li}^* \rightarrow {}^5\text{Li} \rightarrow \alpha + p$	$28.1 \pm 4.0$	19.2	$6.8 \pm 1.0$	7.9
${}^6\text{Li}^* \rightarrow {}^8\text{Be} \rightarrow \alpha + \alpha$	$4.2 \pm 0.8$	4.79	$2.3 \pm 0.5$	2.75
Reaction	$1364 \pm 20$	1344	$521 \pm 15$	493

<sup>a</sup>  $E_x \leq 2$  MeV.

<sup>b</sup>  $E_x \leq 1.4$  MeV.

<sup>c</sup>  $E_x \leq 8$  MeV.

contributing to  $\alpha$  productions, along with total reaction cross sections obtained from optical model fit to elastic scattering, are also given in Table I to understand the underlying reaction mechanisms. For the  ${}^6\text{Li}+{}^{209}\text{Bi}$  system [3], it was observed that the major channels producing  $\alpha$  particles are (i) breakup of  ${}^6\text{Li} \rightarrow \alpha + d$  followed by  $d$  capture (incomplete fusion), (ii) direct and resonant noncapture breakup of  ${}^6\text{Li} \rightarrow \alpha + d$ , and (iii)  $1n$  stripping ( ${}^6\text{Li}, {}^5\text{Li}$ ) followed by breakup, i.e.,  ${}^5\text{Li} \rightarrow \alpha + p$ . In addition to the last two noncapture breakup channels, cross sections for another important  $\alpha$  producing channel, i.e.,  $1d$  pickup ( ${}^6\text{Li}, {}^8\text{Be}$ ) followed by breakup i.e.,  ${}^8\text{Be} \rightarrow \alpha + \alpha$ , have also been measured for the present system. In this channel, both the outgoing fragments being  $\alpha$ , the  $\alpha$  yields become double the number of actual events. The angle integrated cross sections obtained from the CDCC and CRC calculations for noncapture breakup channels are compared with the measured values. The sum of the calculated  $\alpha + d$ ,  $\alpha + p$ , and  $\alpha + \alpha$  cross sections is only  $\sim 15\%$  ( $\sim 12\%$ ) of inclusive  $\alpha$  cross sections at 30 (22) MeV. A contamination from evaporated  $\alpha$  from the compound nucleus is also estimated using statistical model calculations and found to be  $\sim 78\%$ . So, the major contribution of  $\alpha$  may be from the processes like breakup of  ${}^6\text{Li} \rightarrow \alpha + d$  followed by  $d$  capture as observed in Ref. [3],  $1p$  stripping followed by breakup into  $\alpha + n$ , etc. The experimental data on these channels in the future would provide further details of  $\alpha$  production reaction mechanism.

In summary, the major projectile-breakup channels observed in the  ${}^6\text{Li}+{}^{112}\text{Sn}$  reaction at  $E_{\text{beam}} = 30$  and 22 MeV are (i) direct and sequential breakup of  ${}^6\text{Li} \rightarrow \alpha + d$ , (ii) sequential breakup via  $1n$  stripping followed by breakup into  $\alpha + p$ , and (iii) sequential breakup via  $1d$  pickup followed by breakup into  $\alpha + \alpha$ . Sequential  $\alpha + d$  breakup

cross sections of  ${}^6\text{Li}$  via its resonant state ‘ $1^+$ ’ along with ‘ $2^+$ ’, and ‘ $3^+$ ’ in the continuum have been measured for the first time. Breakup via the  $3^+$  state of  ${}^6\text{Li}$  in the continuum, dominates the total  $\alpha + d$  breakup cross section at  $E_{\text{beam}} = 30$  MeV. However, at  $E_{\text{beam}} = 22$  MeV, only direct breakup of  ${}^6\text{Li}$  into  $\alpha + d$  is observed. The breakup channels proceeding via  $1n$  and  $1d$  transfer reactions are observed at both the energies. The  $Q$  value and relative energy spectra show that  $\alpha + p$  breakup proceeds via the same excitations at both the beam energies. However, for the  $\alpha + \alpha$  channel, the breakup at  $E_{\text{beam}} = 22$  MeV proceeds only through the  $0^+$  state of  ${}^8\text{Be}$  whereas at  $E_{\text{beam}} = 30$  MeV it proceeds through both  $0^+$  and  $2^+$  states of  ${}^8\text{Be}$ . Excellent agreement between CDCC calculations and experimental  $\alpha + d$  breakup cross sections via three resonance states of  ${}^6\text{Li}$  confirms the observation of sequential breakup via the resonance state of  $1^+$  along with  $3^+$  and  $2^+$  states. A comparison of breakup cross sections at two energies reveals that the cross sections for  $\alpha + d$  breakup are more than  $\alpha + p$  as well as  $\alpha + \alpha$  breakup. All the breakup channels observed in the present measurements produce  $\alpha$  as one of the two fragments and contribute to total inclusive  $\alpha$  yield. Two additional channels, i.e.,  $\alpha + d$  breakup followed by  $d$  capture and  $1p$  transfer followed by  $\alpha + n$  breakup are expected to have significant contributions in inclusive  $\alpha$ .

The elaborate set of experimental data and theoretical calculations presented here on different breakup channels including the newly found resonant breakup via  $1^+$  state provides a deep insight of the reaction mechanisms involving a weakly bound projectile like  ${}^6\text{Li}$ . Understanding the above reaction mechanisms is an important step in exploring similar reactions involving light radioactive ion beams from upcoming facilities.

- 
- [1] P. K. Rath, S. Santra, N. L. Singh, B. K. Nayak, K. Mahata, R. Palit, K. Ramachandran, S. K. Pandit, A. Parihari, A. Pal *et al.*, *Phys. Rev. C* **88**, 044617 (2013).
- [2] S. Santra, S. Kailas, K. Ramachandran, V. V. Parkar, V. Jha, B. J. Roy, and P. Shukla, *Phys. Rev. C* **83**, 034616 (2011).
- [3] S. Santra, S. Kailas, V. V. Parkar, K. Ramachandran, V. Jha, A. Chatterjee, P. K. Rath, and A. Parihari, *Phys. Rev. C* **85**, 014612 (2012).
- [4] K. O. Pfeiffer, E. Speth, and K. Bethge, *Nucl. Phys. A* **206**, 545 (1973).
- [5] R. Ost, K. Bethge, H. Gemmeke, L. Lassen, and D. Scholz, *Z. Phys.* **266**, 369 (1974).
- [6] D. Scholz, H. Gemmeke, L. Lassen, R. Ost, and K. Bethge, *Nucl. Phys. A* **288**, 351 (1977).
- [7] C. M. Castaneda, H. A. Smith, Jr., P. P. Singh, and H. Karwowski, *Phys. Rev. C* **21**, 179 (1980).
- [8] C. Signorini, M. Mazzocco, G. Prete, F. Soramel, L. Stroe, A. Andrighetto, I. Thompson, A. Vitturi, A. Brondi *et al.*, *Eur. Phys. J. A* **10**, 249 (2001).
- [9] C. Signorini, A. Edifizi, M. Mazzocco, M. Lunardon, D. Fabris, A. Vitturi, P. Scopel, F. Soramel, L. Stroe *et al.*, *Phys. Rev. C* **67**, 044607 (2003).
- [10] J. L. Quebert, B. Frois, L. Marquez, G. Soubie, R. Ost, K. Bethge, and G. Gruber, *Phys. Rev. Lett.* **32**, 1136 (1974).
- [11] A. Shrivastava, A. Navin, N. Keeley, K. Mahata, K. Ramachandran, V. Nanal, V. Parkar, A. Chatterjee, and S. Kailas, *Phys. Lett. B* **633**, 463 (2006).
- [12] A. Diaz-Torres, I. J. Thompson, and C. Beck, *Phys. Rev. C* **68**, 044607 (2003).
- [13] D. R. Tilley, C. M. Cheves, J. L. Godwin, G. M. Hale, H. M. Hofmann, J. H. Kelley, C. G. Sheu, and H. R. Weller, *Nucl. Phys. A* **708**, 3 (2002).
- [14] S. K. Pandit, A. Shrivastava, K. Mahata, N. Keeley, V. V. Parkar, P. C. Rout, K. Ramachandran, I. Martel, C. S. Palshetkar, A. Kumar *et al.*, *Phys. Rev. C* **93**, 061602(R) (2016).
- [15] D. H. Luong, M. Dasgupta, D. J. Hinde, R. du Rietz, R. Rafiei, C. J. Lin, M. Evers, and A. Diaz-Torres, *Phys. Rev. C* **88**, 034609 (2013).
- [16] R. J. de Meijer and R. Kamermans, *Rev. Mod. Phys.* **57**, 147 (1985).
- [17] S. Santra, V. V. Parkar, K. Ramachandran, U. K. Pal, A. Shivastava, B. J. Roy, B. K. Nayak, A. Chatterjee, R. K. Choudhury, and S. Kailas, *Phys. Lett. B* **677**, 139 (2009).
- [18] H. Fuchs, *Nucl. Instrum. Methods* **200**, 361 (1982).

- [19] I. J. Thompson, *Comp. Phys. Rep.* **7**, 167 (1988).
- [20] F. G. Perey and G. R. Satchler, *Nucl. Phys. A* **97**, 515 (1967).
- [21] M. Avrigeanu and V. Avrigeanu, *Phys. Rev. C* **73**, 038801 (2006).
- [22] H. An and C. Cai, *Phys. Rev. C* **73**, 054605 (2006).
- [23] E. J. Schneid, A. Prakash, and B. L. Cohen, *Phys. Rev.* **156**, 1316 (1967).
- [24] P. L. Kerr, K. W. Kemper, P. V. Green, K. Mohajeri, E. G. Myers, and B. G. Schmidt, *Phys. Rev. C* **55**, 2441 (1997).
- [25] P. J. Blankert, H. P. Blok, and J. Blok, *Nucl. Phys. A* **356**, 74 (1981).